Atherosclerosis 273 (2018) 106–114

Contents lists available at ScienceDirect

Atherosclerosis

journal homepage: www.elsevier.com/locate/atherosclerosis

Ex vivo vessel wall thickness measurements of the human circle of Willis using 7T MRI

Anita A. Harteveld [a, *], Nerissa P. Denswil [b], Wim Van Hecke [c], Hugo J. Kuijf [d], Aryan Vink [c], Wim G.M. Spliet [c], Mat J. Daemen [b], Peter R. Luijten [a], Jaco J.M. Zwanenburg [a], Jeroen Hendrikse [a], Anja G. van der Kolk [a]

[a] Department of Radiology, University Medical Center Utrecht, Postbox 85500, 3508 GA, Utrecht, The Netherlands
[b] Department of Pathology, Academic Medical Center, Postbox 22660, 1100 DD, Amsterdam, The Netherlands
[c] Department of Pathology, University Medical Center Utrecht, Postbox 85500, 3508 GA, Utrecht, The Netherlands
[d] Image Sciences Institute, University Medical Center Utrecht, Postbox 85500, 3508 GA, Utrecht, The Netherlands

ARTICLE INFO

Article history:
Received 17 January 2018
Received in revised form
30 March 2018
Accepted 18 April 2018
Available online 24 April 2018

Keywords:
Atherosclerosis
Brain
Cerebral circulation
Magnetic resonance imaging
Vessel wall
Wall thickness

ABSTRACT

Background and aims: MRI can detect intracranial vessel wall thickening before any luminal stenosis is present. Apart from representing a vessel wall lesion, wall thickening could also reflect normal (age-related) variations in vessel wall thickness present throughout the intracranial arterial vasculature. The aim of this study was to perform vessel wall thickness measurements of the major intracranial arteries in *ex vivo* circle of Willis (CoW) specimens using 7T MRI, to obtain more detailed information about wall thickness variations of the intracranial arteries.

Methods: Fifteen human CoW specimens were scanned at 7T MRI with an ultrahigh-resolution T_1-weighted sequence. Five specimens were used for validation of MRI measurements with histology and evaluation of inter-rater reliability and agreement. The other 10 specimens from patients with ($n = 5$) and without ($n = 5$) cerebrovascular disease were used for vessel wall thickness measurements over the entire length of the major arterial segments of the CoW using MRI only.

Results: MRI measurements showed excellent agreement with histology. Mean wall thickness varied from 0.45 to 0.66 mm, minimum wall thickness from 0.31 to 0.42 mm, maximum wall thickness from 0.52 to 0.86 mm, and normalized wall index from 0.64 to 0.75. On average, vessel walls were thicker for symptomatic patients compared to asymptomatic patients.

Conclusions: High-resolution MRI enables accurate measurement of vessel wall thickness in *ex vivo* CoW specimens. Vessel wall thickness measurements over the entire length of segments showed considerable variation both within and between arterial segments of patients.

1. Introduction

In the last decade, several MRI sequences have been developed for direct visualization of the intracranial vessel wall [1]. Their advantage, compared with conventional imaging techniques for visualization of the intracranial arteries (e.g. MRA or CTA), is the ability to detect vessel wall lesions before any luminal stenosis is present [2]. A vessel wall lesion is generally defined as a focal or more diffuse but restricted area of vessel wall thickening. However, apart from representing a vessel wall lesion, wall thickening could also reflect normal (age-related) variation in vessel wall thickness present throughout the intracranial arterial vasculature.

Currently, differentiation between pathological thickening and normal (age-related) vessel wall thickness variation is difficult. Autopsy studies have described the spatial distribution and severity of atherosclerosis in the intracranial arteries [3–5]. However, in contrast to vessel wall (intima-media) thickness of extracranial arteries, which have been studied more extensively thus far, limited information is available on the quantitative assessment of vessel wall thickness and thickness variation over entire arterial segments of the arteries of the circle of Willis (CoW) [6–9]. This is mainly because the intracranial arteries are small and have a tortuous orientation, which demands high quality (both with respect to contrast-to-noise and spatial resolution) of the used imaging

* Corresponding author.
E-mail address: a.a.harteveld-2@umcutrecht.nl (A.A. Harteveld).

https://doi.org/10.1016/j.atherosclerosis.2018.04.023

techniques to properly visualize the vessel wall *in vivo*. In addition, the arteries are difficult to access, hampering correlation of *in vivo* imaging results with histology [10]. Next to differentiating normal thickness variation from vessel wall lesions, information regarding wall thickness would also shed new light on the minimum spatial resolution required for dedicated *in vivo* vessel wall imaging. MR imaging of *ex vivo* specimens enables visualization of these small and tortuous intracranial arteries with ultra-high spatial resolution from which thickness measurements over the entire length of arterial segments can be derived, combined with histologic validation to distinguish between pathological thickening and normal vessel wall thickness. In histological assessments, normally only a limited number of samples are analyzed per vessel segment. *Ex vivo* MRI with ultra-high spatial resolution allows for assessment of entire arterial segments to examine total vessel wall thickening/lesion burden, thereby posing a viable complementary method to histological assessment [11].

In the current study, vessel wall thickness measurements of the major intracranial arteries were performed in *ex vivo* specimens of the CoW using 7T MRI, to obtain more detailed information about wall thickness variations of the intracranial arteries. Histology was used for validation of the MRI measurements. Thickness measurements were performed in patients with and without cerebrovascular disease, obtaining an impression of vessel wall thickness variations present in different patient subgroups.

2. Materials and methods

2.1. Specimens

Human CoW specimens were selected for this study from >100 autopsy cases that were performed in our institution. For validation of MRI measurements with histology, specimens were used that had been selected for a previous study on plaque characteristics [12]. For the other specimens used in this study, patients with a clinical history of TIA or ischemic stroke (further referred to as 'symptomatic' patients), and without a clinical history of cerebrovascular disease (further referred to as 'asymptomatic' patients) were selected, to enable comparison of vessel wall thickness in both populations.

Institutional review board approval was obtained for this retrospective study. The material was handled in a coded manner that met the criteria of the Code of conduct used in the Netherlands for responsible use of human tissue in medical research (www.federa.org/codes-conduct).

2.1.1. Specimen preparation

All specimens were stored in buffered formalin (4%). Before scanning, all specimens were cleaned from clotted blood products and embedded in a petri dish containing 2% agarose solution, as previously described [13]. To enable spatial correlation between MR images and histological slides for validation of MRI measurements, fiducials (cactus spines) were placed in the agarose gel at 15 locations adjacent to an arterial segment in each CoW specimen. The locations were chosen to sample all major arterial segments of the CoW including their branches (Fig. 1A) [12].

2.2. MR imaging

Imaging was performed at room temperature on a 7T whole body system (Philips Healthcare, Best, the Netherlands), with a custom-made high-density receive coil (16 channels per 70 cm^2; MR Coils BV, Zaltbommel, the Netherlands) [14], and a volume transmit/receive coil for transmission (Nova Medical, Wilmington, MA, USA). The embedded specimens used for validation were imaged individually; the petri dish containing the specimen was placed in the middle of the transmit/receive coil on top of the high-density receive coil. The other specimens (without histopathological validation) were imaged two at a time, with two high-density receive coils placed above and below the two petri dishes containing the specimens.

2.2.1. Protocol

All specimens were scanned with an ultra-high resolution 3D T_1-weighted gradient echo sequence with short TR and relatively high flip angle for T_1 weighting. In a previous *ex vivo* study at 7T [12], T_1-weighted imaging was shown to have the most promising image contrast for visualizing the intracranial arterial vessel wall. The five specimens used for validation were scanned with the following scan parameters [12]: FOV $150 \times 150 \times 20$ mm^3, acquired resolution $0.13 \times 0.13 \times 0.13$ mm^3, TR/TE 16/4.3 ms, flip angle 44°, bandwidth 165 Hz/pixel, 1154 ky-lines per shot, acquisition time approximately 1h35min per specimen. The other ten specimens were scanned with a sequence with an even higher spatial resolution [13], optimized for the vessel wall T_1 relaxation times reported previously at 7T [12]: FOV $95 \times 130 \times 35$ mm^3, acquired resolution $0.11 \times 0.11 \times 0.11$ mm^3, TR/TE 55/6.1 ms, flip angle 28°, bandwidth 184 Hz/pixel, 1182 ky-lines per shot, acquisition time approximately 5h46min for two specimens. To mitigate potential artifacts caused by scanner frequency drift, the scanner resonance frequency was measured and adjusted between each shot during scanning. The isotropic resolution of the acquired MR images allowed for reconstructions along arbitrary planes.

2.3. Validation of MRI measurements with histology

After scanning, samples were taken from the 15 marked locations of each CoW specimen that was used for validation. Each sample was marked with ink for spatial orientation after histological processing. Histological processing was performed using an in-house developed protocol, as previously described [13]. From the MR images MPRs were made (interslice distance: 0.5 mm) perpendicular to the centerline of the artery (drawn manually) at the fiducial locations, using dedicated vascular analysis software (Cardiovascular Angiographic Analysis System (CAAS) MRA; Pie Medical Imaging, Maastricht, The Netherlands). Next, the MR and histological images were matched manually by one rater (AH) using the ink markings in the histological sections, the locations marked with the fiducials in the MR images, and the gross morphological features. Samples were excluded from validation when: (1) no match was found, (2) the histological section was too fragmented, or (3) air bubbles were present in the MR images.

After matching the histological sections with the corresponding MR images, vessel wall boundaries (outer wall and lumen contours) were drawn in the histological sections by one rater (AH) blinded to the MRI data, and vice versa (Fig. 1). Splits present in the vessel wall due to the histological preparation procedure were taken into account by drawing separate ROIs for each split, and adding these areas to the lumen area. Total vessel and lumen area derived from the drawn vessel wall contours were used for comparison of MRI measurements with histology.

2.4. Vessel wall thickness analysis

For the histological sections, vessel wall boundaries were drawn manually using MeVisLab (version 2.7; MeVis Medical Solutions, Bremen, Germany; Fig. 1C). For the MRI slices, vessel wall boundaries were drawn on the reconstructed images using the software program CAAS MRA, with dedicated add-on software MRTool (Fig. 1D). Based on the manually traced vessel boundary contours,

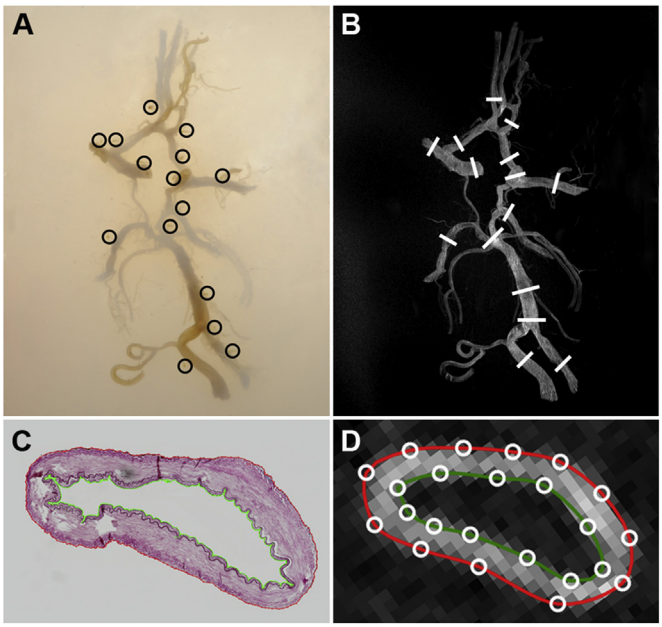

Fig. 1. Example of one of the circle of Willis specimens used for validation of the vessel wall thickness measurements.
(A) Photograph and (B) T_1-weighted image (maximum intensity projection). The black circles in (A) indicate fiducials (cactus spines) placed for spatial correlation at 15 locations along the major arterial segments of the circle of Willis. The white markings in (B) show the locations used for histological sampling and multiplanar reconstructions of MR images. (C) Histological section of a sample from the specimen (right vertebral artery) with the corresponding T_1-weighted image (D), showing the manually drawn vessel wall boundaries of the outer wall (red) and lumen (green) from which the vessel wall thickness parameters were calculated. The white circles in (D) indicate the manually placed points by the rater to delineate the vessel wall boundaries, which can be manually adjusted retrospectively with the used software program if necessary. (For interpretation of the references to colour in this figure legend, the reader is referred to the Web version of this article.)

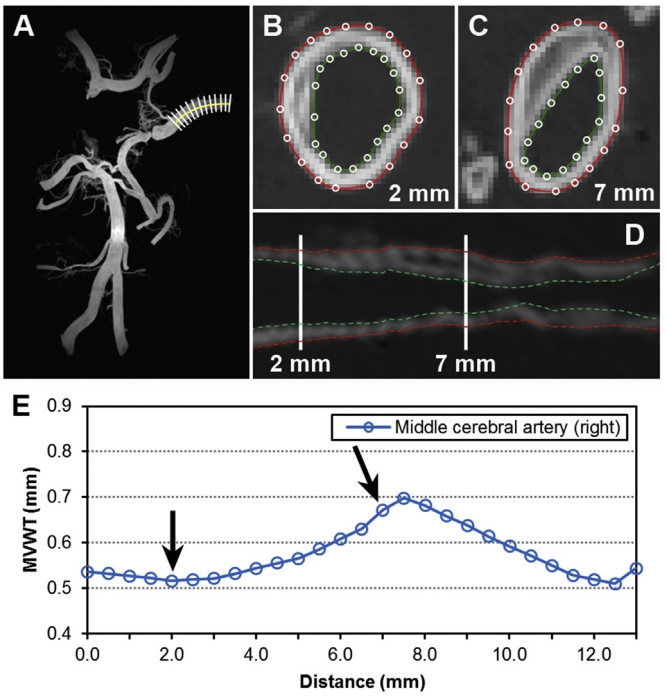

Fig. 2. Calculation of vessel wall thickness parameters based on the drawn vessel wall boundaries.
(A) T_1-weighted image (maximum intensity projection) of an embedded circle of Willis specimen used for MRI-based vessel wall thickness assessment over the entire length of different vessel segments. The white markings show the multiplanar reconstructions (MPRs) that were made perpendicular to the centerline (yellow line) for the right middle cerebral artery. Examples of MPR images at 2 mm (B) and 7 mm (C) showing the vessel wall boundaries delineated for the outer wall (red) and lumen (green). (D and E) Based on the drawn vessel wall boundaries in each reconstructed slice, vessel wall thickness parameters were calculated for the entire arterial segment. (For interpretation of the references to colour in this figure legend, the reader is referred to the Web version of this article.)

vessel wall parameters were calculated by the software programs for each analyzed slice (for MRI and histology separately). These parameters included: lumen area (LA), total vessel area (TVA), wall area (WA; TVA-LA), wall thickness (mean, minimum, and maximum), and normalized wall index (WA/TVA). The mean vessel wall thickness was calculated based on the vessel areas [15]. In this method mean vessel wall thickness for each slice is calculated as the difference in the radii of the total vessel and lumen area (Fig. 2 of Ref [16]). Minimum and maximum wall thickness were calculated as the minimal and maximal distance measured between outer wall and luminal boundary. Distance between outer wall and luminal boundary were automatically determined at multiple locations ($\geq$100) by the used software programs.

Inter-rater reliability and agreement of the calculated vessel wall parameters were assessed using vessel wall boundaries drawn by a second rater (AK) in a subset of the histological sections and their matching MRI slices.

2.4.1. MRI measurements of arterial segments

Vessel wall thickness measurements were performed over the entire length of the major arterial segments of the CoW, using the CAAS MRA software, blinded to the clinical history of the patients. First, MPRs were made perpendicular to the centerline of each arterial segment (interslice distance: 1.0 mm). Next, vessel wall boundaries (outer wall and lumen) were drawn in each reconstructed slice by one rater (AH). Based on the drawn vessel wall boundaries, vessel wall thickness parameters were calculated (Fig. 2). All segments were analyzed from proximal to distal, and over a fixed length for all specimens (longest length possible to still include the majority of subjects). The analyzed vessel segments included: anterior cerebral artery (A1 segment, length: 10 mm; A2 segment, length: 5 mm), intracranial internal carotid artery (C7 segment, length: 4 mm), middle cerebral artery (M1 segment, length: 7 mm), basilar artery (proximal part, length: 9 mm; distal part, length: 9 mm), posterior cerebral artery (P1 and P2 segments, length: 8 mm), and vertebral artery (length: 12 mm). The posterior communicating arteries were not assessed based on their known variability in size/presence. Hypoplastic vessel segments, slices containing side branches originating from the artery of interest (possibly resulting in overestimation of thickness measurements), or vessel segments/slices where the vessel wall contours were not well visible (e.g. due to air present in the arterial lumen or collapsed vessel) were excluded from thickness calculations. Linear interpolation of calculated vessel wall thickness parameters was performed for the vessel walls located in between the reconstructed slices, as well as for the excluded slices.

2.5. Statistical analysis

MRI measurements of vessel wall parameters were compared with the histological measurements by linear regression analysis. Inter-rater reliability and agreement of the derived vessel wall parameters were evaluated using the intraclass correlation coefficient and Bland-Altman analysis. Mean and standard deviation values for the vessel wall parameters were calculated for each

included segment (with fixed length) over all specimens, and for the individual slices over the entire length of each segment (grouped for asymptomatic and symptomatic patients).

3. Results

3.1. Specimens

In total, 15 CoW specimens were included in this study. Five specimens (from 5 patients) were used for validation of MRI measurements with histology and evaluation of inter-rater reliability and agreement (3 male; mean age 66.2 years; range 42–92 years). The other 10 specimens from patients with (n = 5) and without (n = 5) cerebrovascular disease were used for vessel wall thickness measurements over the entire length of the major arterial segments of the CoW using MRI only. Demographic and clinical data of these specimens are summarized in Table 3 of [16].

3.2. Validation of MRI measurements with histology

From the five CoW specimens that were selected for validation of MRI measurements with histology, in total 70 samples were obtained from the different arterial segments (15 marked locations per specimen, Fig. 1A and B; n = 5 arterial segments were absent). Of these samples, 25 were excluded due to: (1) lack of match between the MR image and histological section (n = 8), (2) fragmentation of the histological section (n = 16), or (3) the presence of air on MRI (n = 1), leaving 45 samples for validation analysis. The lack of match between MRI and histology is probably mainly caused by deformation of the histological section after removing the sample from the embedded specimen for histological processing. On average 9 samples were included per specimen (range 7–10).

Scatterplots and Bland-Altman plots of lumen and total vessel area measurements on the histological sections and corresponding MR images are shown in Fig. 3. The total vessel and lumen areas measured on MRI both had a high goodness-of-fit with histology, ($R^2 = 0.95$ and $R^2 = 0.91$, respectively), with a root-mean-square-error of 1.02 mm^2 and 0.62 mm^2, respectively. Furthermore, Bland-Altman plots (Fig. 3C and D) showed a positive bias for MRI measurement relative to histology measurement for both total vessel and lumen area (0.71 mm^2 and 0.35 mm^2, respectively).

Inter-rater reliability of parameters derived from the delineated vessel wall boundaries in a subset of 10 samples (22%) was excellent for both MRI and histology; all intraclass correlation coefficients were above 0.85 (Table 2 of [16]).

3.3. MRI measurements of arterial segments

In the ten specimens selected for MRI-based vessel wall thickness assessment, 123 arterial segments were present (n = 7 segments were absent). Of these 123 segments, 21 were excluded for different reasons: the segment was too short (n = 10), the segment was hypoplastic (n = 5), the vessel had collapsed (n = 4), or the presence of air in the lumen (n = 2). This resulted in a total of 102 vessel segments that were included for analysis (52 from asymptomatic patients; 50 from symptomatic patients).

Segment averages of thickness measurements from all patients are presented in Table 1 of [16]. Thickness measurements over the entire length of each analyzed vessel segment are shown in Fig. 4 (mean wall thickness) and Fig. 5 (minimum and maximum wall thickness), grouped for the asymptomatic and symptomatic patients. In Fig. 1 of [16], mean vessel wall thickness MRI measurements over the entire vessel segment are shown for each individual patient.

4. Discussion

The current study focused on vessel wall thickness measurements of the major intracranial arteries, measured using 7T MRI in both asymptomatic and symptomatic patients. The main results show that ultrahigh-resolution MRI at 7T enables accurate measurement of vessel wall thickness in *ex vivo* CoW specimens with excellent agreement with histology. Vessel wall thickness measurements over entire segments showed considerable variation both within and between arterial segments of patients. Symptomatic patients on average had thicker walls than asymptomatic patients.

The number of studies performing vessel wall thickness measurements of the intracranial arteries *in vivo* is still limited. Thus far, studies have mainly focused on performing thickness measurements in patients at the location of a stenosis in a specific arterial segment, like the middle cerebral artery [17–19] or basilar artery [20,21], or at standard locations representing common sites for intracranial atherosclerosis in healthy controls and patients [22]. Difficulties encountered during *in vivo* measurements were delineation of the outer wall at the interface between vessel wall and brain parenchyma, although this improved in patients with more CSF surrounding the arteries due to age-related brain atrophy [18]. In addition, the choice of a good reference site was often stated to be difficult [18,20]. Recently, a large multicenter study by Qiao et al. [23] included *in vivo* quantitative measurements of several intracranial vessel segments. Measurements were performed over a longer distance for each analyzed vessel segment, instead of only focusing on a specific location (i.e. stenosis). Their measured mean vessel wall thickness ranged from 0.95 (basilar artery; average white participants) to 1.05 mm (anterior cerebral artery; average white participants). In the current study this ranged from 0.45 (anterior cerebral artery (A1 segment)) to 0.66 mm (internal carotid artery) when taking into account vessel segments that were included in both studies.

One of the major drawbacks of *ex vivo* studies is the effect of tissue storage. Formalin used for tissue fixation causes some tissue shrinkage, which ranges from 8 to 20% [24,25]. This shrinkage partially covers the observed significant difference in mean vessel wall thickness between *in vivo* [23] and the *ex vivo* measurements reported here, where the mean vessel wall thickness is ~50% smaller *ex vivo* than *in vivo*. Another important factor possibly explaining the difference between *ex vivo* and *in vivo* studies, such as that by Qiao et al. [23], is the spatial resolution that was used for acquisition of the vessel wall images. The reported *in vivo* acquired spatial resolution was $0.5 \times 0.5 \times 0.5$ mm^3. To perform accurate thickness measurements, at least two full voxels without partial volume effects should represent the vessel wall (Nyquist-Shannon sampling theorem) [26,27]. Taking into account the diagonal of voxels, this results in a minimum thickness of (sqrt(3) * .5 * 2 =) 1.7 mm to ensure reliable results regardless of the orientation of the vessel with respect to the voxels. Assuming the wall is parallel to one of the voxel faces, the minimum reliable thickness is still 1.0 mm. In the study by Qiao et al., the mean vessel wall thickness for all analyzed segments varies closely around this minimum thickness of 2 voxels, while in the current postmortem study thickness was measured with a much higher spatial resolution ($0.11 \times 0.11 \times 0.11$ mm^3) resulting in lower values with more variation between the different vessel segments (0.45–0.66 mm). Finally, another important factor that could explain differences between *in vivo* and *ex vivo* thickness measurements is the occurrence of radial and transitional displacements of the vessel wall during the cardiac cycle. This can limit *in vivo* measurement of vessel wall boundaries and subsequently wall thickness.

Although there was considerable variation between individual

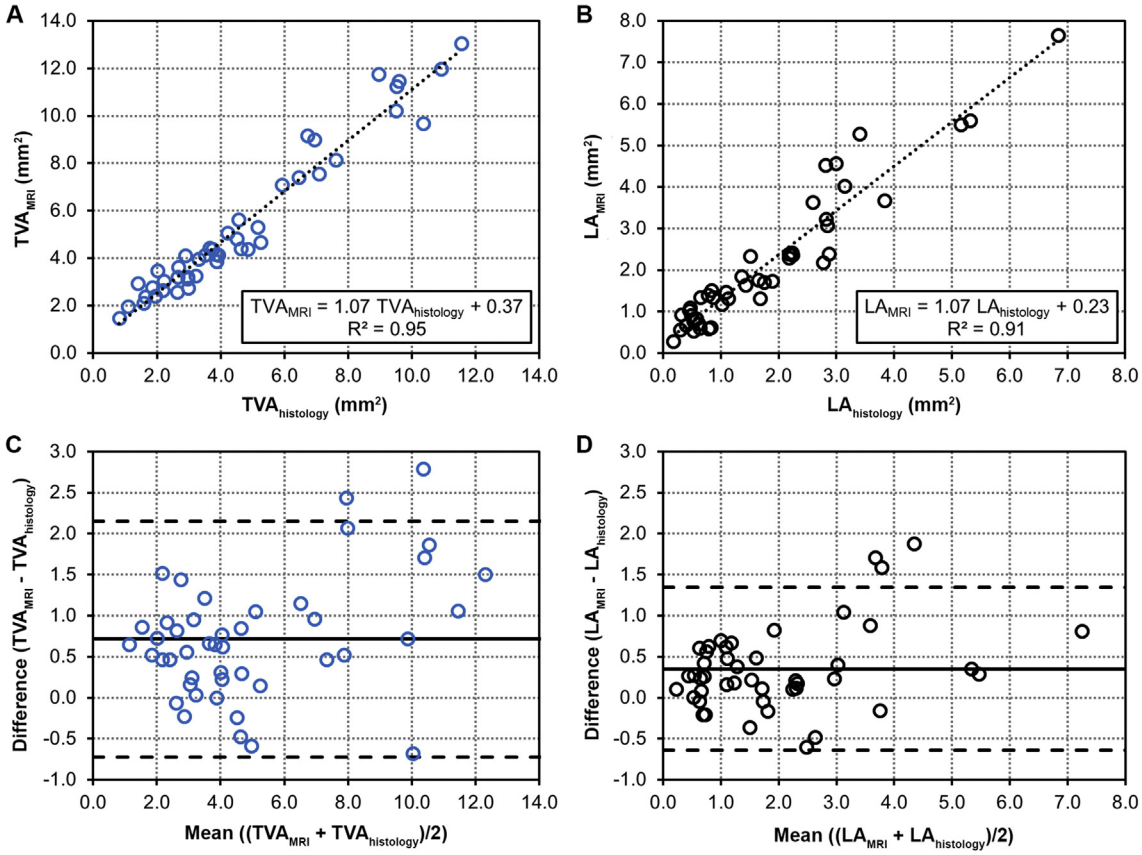

Fig. 3. Scatterplots and Bland-Altman plots of total vessel and lumen area measurements on the histological sections and corresponding MR images.
(A and C) Total vessel area (TVA) and (B and D) lumen area (LA) measurements derived from the drawn vessel wall contours for the outer wall and lumen.

patients, on average the vessel wall showed more thickening for the symptomatic group compared with the asymptomatic group for all analyzed segments. Thus far, asymptomatic and symptomatic patients have only been compared *in vivo* at the location of an MCA stenosis [17,19]. A previous autopsy study showed intracranial atherosclerosis was more frequently present in (fatal) stroke patients than in their control group (without stroke) [28], which might be an explanation for the increased wall thickness in our symptomatic group. Other vascular territories have already been studied more extensively. For instance, increased vessel wall (intima-media) thickness in the carotid artery [29] and aorta [30] was found to be associated with future cardiovascular events. Studies in a healthy general population or without clinical cardiovascular disease showed wall thickness increases with age and varies with sex and race [7,31].The prevalence of intracranial atherosclerosis has also been shown to vary depending on race-ethnicity, sex and age [32,33]. In the current study, the number of included patients was not large enough to stratify between different characteristics to identify the driving factor of the difference in wall thickness observed both within and between the two groups. A future study in a larger patient population with different risk factors and cerebrovascular disease burden would be an interesting next step towards a better understanding of possible causes of increased vessel wall thickness of the intracranial arteries.

The number of excluded samples for validation of MRI measurements with histology was relatively high. Fortunately, the excluded samples were relatively equally spread over the different arterial segments. Only the number of excluded vertebral artery samples was notable (7/10), however, this was mainly because this arterial segment was often absent (n = 5). Also the number of excluded samples of the ICA was relatively high. For this segment it was often difficult to obtain a proper sample for histological processing, since the excision length performed by the pathologist during autopsy was often very short. Because a large number of samples were obtained per specimen from multiple arterial segments, the included samples still represent a wide range of arterial segments from multiple specimens.

Several limitations exist in this study. First, the number of patients in this study is relatively small. Therefore, differences observed between groups in this study should be further investigated in future studies within a larger patient population. Second, image analysis was performed manually. Especially delineation of the lumen and outer wall contours over entire segments was very labor- and time intensive. Development of a tool that is capable of performing vessel wall delineation automatically, as is available for the carotid arteries and descending aorta [34], would be a prerequisite when expanding to larger patient groups. Third, the fixed length that was used for each included arterial segment in this study was determined by the excision lengths performed by the pathologist during brain autopsy. To include more data over longer distances in future studies, the variation in excision lengths between specimens should be reduced. Fourth, wall thickness differences between specimens could be influenced by the presence of focal atherosclerotic plaques as opposed to diffuse thickening of the walls. However, because of the focal nature of these plaques, we expect the maximum wall thickness would have been influenced primarily, while their effect would have been dampened in the mean thickness calculations. Fifth, patients in this study were subdivided in groups based on a clinical history of TIA/ischemic stroke (symptomatic) or the absence of a clinical history of

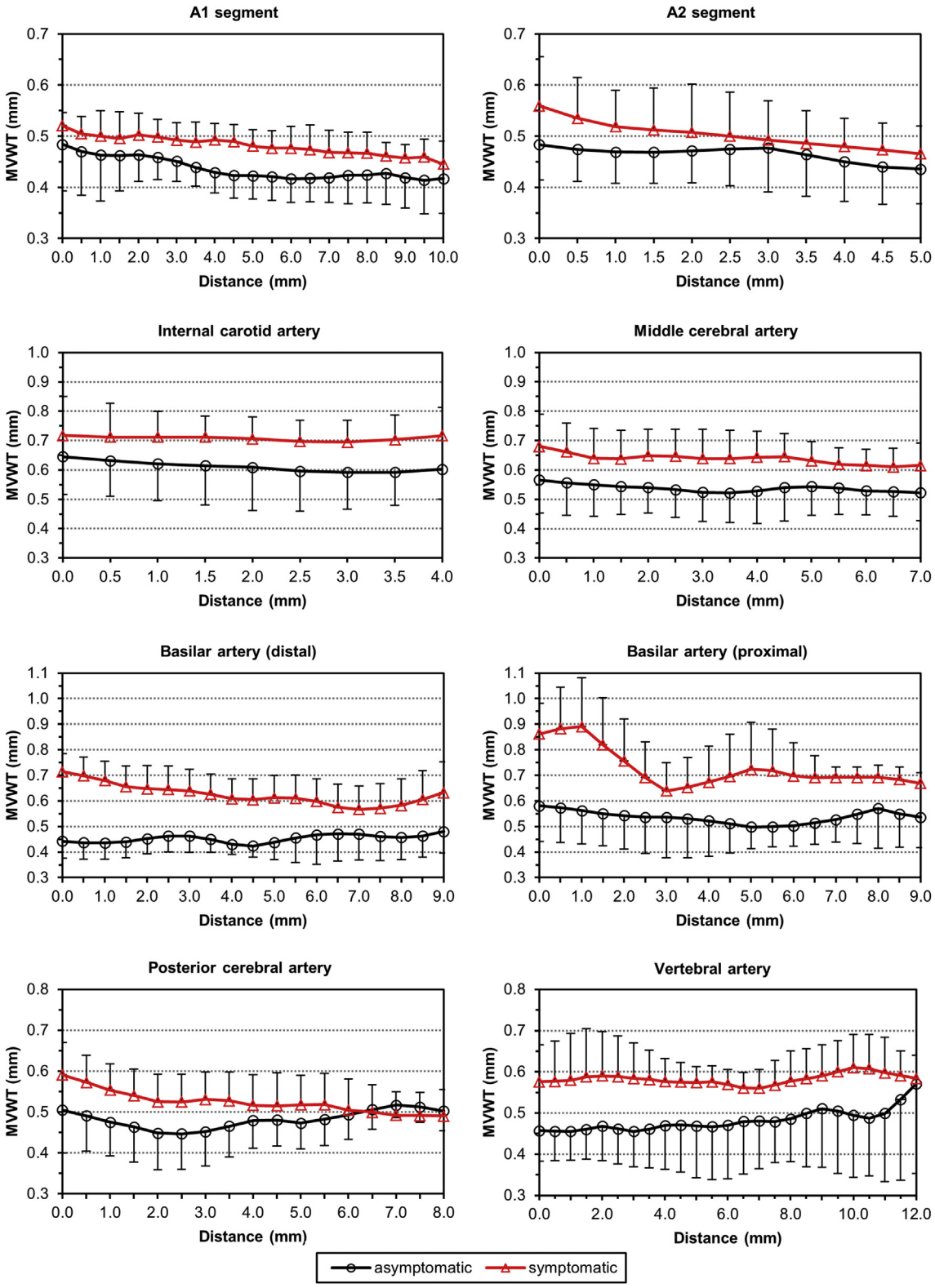

Fig. 4. Mean vessel wall thickness (MVWT) MRI measurements over the fixed length of each analyzed vessel segment.
For set locations along the length of the arterial segments (sample distance: 0.5 mm), mean and standard deviation were calculated for the symptomatic (red) and asymptomatic (black) specimens, separately. One-sided error bars are shown for clarity. The distance represents the locations along the arterial segments from proximal to distal. (For interpretation of the references to colour in this figure legend, the reader is referred to the Web version of this article.)

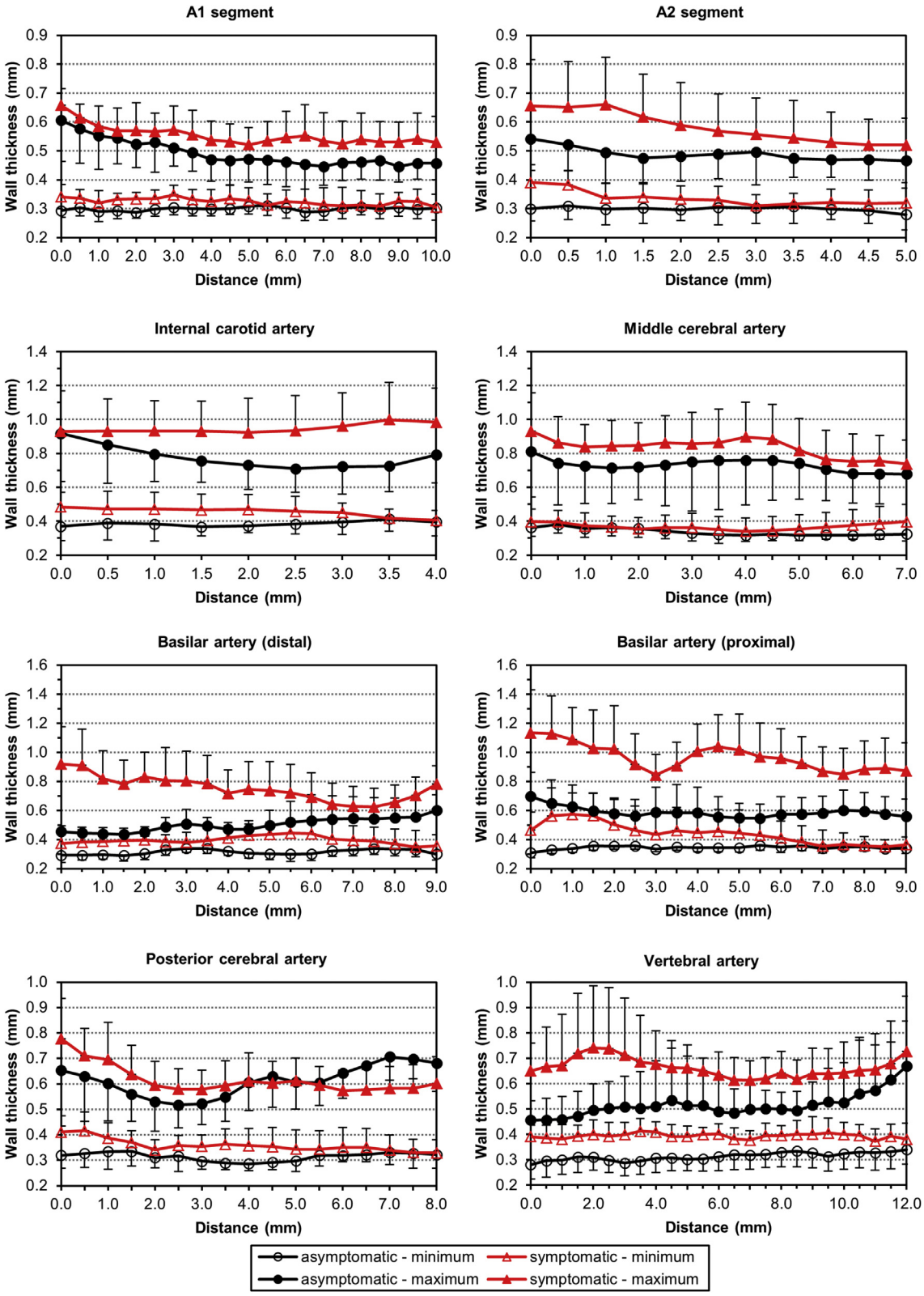

Fig. 5. Minimum and maximum vessel wall thickness MRI measurements over the fixed length of each analyzed vessel segment.
Mean and standard deviation were calculated for the symptomatic (red) and asymptomatic (black) specimens separately, conform to Fig. 4. One-sided error bars are shown for clarity. The distance represents locations along the arterial segments from proximal to distal. (For interpretation of the references to colour in this figure legend, the reader is referred to the Web version of this article.)

cerebrovascular disease (asymptomatic). However, patients without a history of cerebrovascular disease might still have risk factors that play a role in the development of intracranial atherosclerotic plaque formation. For future studies, it might be important to take this into account when comparing different subgroups, to reduce/better explain variation/outliers within groups (e.g. specimen 5 of the asymptomatic group in Fig. 1 of [16]). Lastly, scan sequences with different spatial resolutions were used for the validation with histology ($0.13 \times 0.13 \times 0.13\,mm^3$) and the MRI measurements of arterial segments ($0.11 \times 0.11 \times 0.11\,mm^3$). Increasing spatial resolution has been shown to improve reproducibility of wall dimension measurements [35]. MRI measurements on images with the lower spatial resolution already showed excellent agreement with histology, as well as excellent inter-rater agreement. Therefore, using MR images with even higher spatial resolution will only improve these results.

In conclusion, ultrahigh-resolution MRI enables accurate measurement of vessel wall thickness in *ex vivo* CoW specimens, showing thickness variations over entire segments. The major arteries of the CoW showed thickness variation both within and between arterial segments of patients, as well as between asymptomatic and symptomatic patients. Considering the relatively small thickness variations that are present, the currently used *in vivo* intracranial vessel wall MRI sequences require a higher spatial resolution for accurate measurement of vessel wall thickness in patients and to detect changes over time.

Conflicts of interest

The authors declared they do not have anything to disclose regarding conflict of interest with respect to this manuscript.

Financial support

This work was funded by the Netherlands Organisation for Scientific Research under grant n°91712322 (JH) and the European Research Council under the European Union's Horizon 2020 Programme (H2020)/ERC grant agreement n°637024 (JH) and ERC grant agreement n° 337333 (JZ).

Author contributions

Anita A. Harteveld; study concept and design, acquisition of data, analysis, interpretation of data, and manuscript drafting.

Nerissa P. Denswil; acquisition of data, analysis, and critical revision of manuscript for intellectual content.

Wim Van Hecke; acquisition of data, and critical revision of manuscript for intellectual content.

Hugo J. Kuijf; analysis, and critical revision of manuscript for intellectual content.

Aryan Vink; critical revision of manuscript for intellectual content.

Wim G.M. Spliet; critical revision of manuscript for intellectual content.

Mat J. Daemen; critical revision of manuscript for intellectual content.

Peter R. Luijten; critical revision of manuscript for intellectual content.

Jaco J.M. Zwanenburg; acquisition of data, and critical revision of manuscript for intellectual content.

Jeroen Hendrikse; study concept and design, critical revision of manuscript for intellectual content, and study supervision.

Anja G. van der Kolk; study concept and design, analysis, critical revision of manuscript for intellectual content, and study supervision.

Acknowledgements

The authors would like to acknowledge Jean-Paul Aben and Chris Bouwman from Pie Medical Imaging, The Netherlands, for providing the additional MRTool software specifically designed for this study.

References

[1] N. Dieleman, A.G. van der Kolk, J.J. Zwanenburg, et al., Imaging intracranial vessel wall pathology with magnetic resonance imaging: current prospects and future directions, Circulation 130 (2014) 192–201.
[2] J.D. Bodle, E. Feldmann, R.H. Swartz, et al., High-resolution magnetic resonance imaging: an emerging tool for evaluating intracranial arterial disease, Stroke 44 (2013) 287–292.
[3] J.A. Resch, N. Okabe, R.B. Loewenson, et al., Pattern of vessel involvement in cerebral atherosclerosis. A comparative study between a Japanese and Minnesota population, J. Atherosclerosis Res. 9 (1969) 239–250.
[4] A.B. Baker, A. Iannone, Cerebrovascular disease. I. The large arteries of the circle of Willis, Neurology 9 (1959) 321–332.
[5] N.P. Denswil, A.C. van der Wal, K. Ritz, et al., Atherosclerosis in the circle of Willis: spatial differences in composition and in distribution of plaques, Atherosclerosis 251 (2016) 78–84.
[6] M.W. Lorenz, H.S. Markus, M.L. Bots, et al., Prediction of clinical cardiovascular events with carotid intima-media thickness: a systematic review and meta-analysis, Circulation 115 (2007) 459–467.
[7] B. Mensel, A. Quadrat, T. Schneider, et al., MRI-based determination of reference values of thoracic aortic wall thickness in a general population, Eur. Radiol. 24 (2014) 2038–2044.
[8] T.Z. Naqvi, M.S. Lee, Carotid intima-media thickness and plaque in cardiovascular risk assessment, JACC Cardiovasc Imaging 7 (2014) 1025–1038.
[9] R. Macedo, S. Chen, S. Lai, et al., MRI detects increased coronary wall thickness in asymptomatic individuals: the multi-ethnic study of atherosclerosis (MESA), J. Magn. Reson. Imag. 28 (2008) 1108–1115.
[10] S. Ryoo, J. Cha, S.J. Kim, et al., High-resolution magnetic resonance wall imaging findings of Moyamoya disease, Stroke 45 (2014) 2457–2460.
[11] M.B. Westover, M.T. Bianchi, C. Yang, et al., Estimating cerebral microinfarct burden from autopsy samples, Neurology 80 (2013) 1365–1369.
[12] A.A. Harteveld, N.P. Denswil, J.C. Siero, et al., Quantitative intracranial atherosclerotic plaque characterization at 7T MRI: an ex vivo study with histologic validation, AJNR Am J Neuroradiol 37 (2016) 802–810.
[13] A.G. van der Kolk, J.J. Zwanenburg, N.P. Denswil, et al., Imaging the intracranial atherosclerotic vessel wall using 7T MRI: initial comparison with histopathology, AJNR Am J Neuroradiol 36 (2015) 694–701.
[14] N. Petridou, M. Italiaander, B.L. van de Bank, et al., Pushing the limits of high-resolution functional MRI using a simple high-density multi-element coil design, NMR Biomed. 26 (2013) 65–73.
[15] E.B. Rosero, R.M. Peshock, A. Khera, et al., Agreement between methods of measurement of mean aortic wall thickness by MRI, J. Magn. Reson. Imag. 29 (2009) 576–582.
[16] Harteveld AA, Denswil NP, Van Hecke W, et al: Data on Vessel wall Thickness Measurements of Intracranial Arteries Derived from Human circle of Willis Specimens. Data in Brief; Submitted.
[17] W.H. Xu, M.L. Li, S. Gao, et al., In vivo high-resolution MR imaging of symptomatic and asymptomatic middle cerebral artery atherosclerotic stenosis, Atherosclerosis 212 (2010) 507–511.
[18] X.J. Zhu, B. Du, X. Lou, et al., Morphologic characteristics of atherosclerotic middle cerebral arteries on 3T high-resolution MRI, AJNR Am J Neuroradiol 34 (2013) 1717–1722.
[19] C.W. Ryu, G.H. Jahng, E.J. Kim, et al., High resolution wall and lumen MRI of the middle cerebral arteries at 3 tesla, Cerebrovasc. Dis. 27 (2009) 433–442.
[20] N. Ma, W.J. Jiang, X. Lou, et al., Arterial remodeling of advanced basilar atherosclerosis: a 3-tesla MRI study, Neurology 75 (2010) 253–258.
[21] B. Huang, W.Q. Yang, X.T. Liu, et al., Basilar artery atherosclerotic plaques distribution in symptomatic patients: a 3.0T high-resolution MRI study, Eur. J. Radiol. 82 (2013) e199–203.
[22] Y. Qiao, D.A. Steinman, Q. Qin, et al., Intracranial arterial wall imaging using three-dimensional high isotropic resolution black blood MRI at 3.0 Tesla, J. Magn. Reson. Imag. 34 (2011) 22–30.
[23] Y. Qiao, E. Guallar, F.K. Suri, et al., MR imaging measures of intracranial atherosclerosis in a population-based study, Radiology 280 (2016) 860–868.
[24] T. Tran, C.P. Sundaram, C.D. Bahler, et al., Correcting the shrinkage effects of formalin fixation and tissue processing for renal tumors: toward standardization of pathological reporting of tumor size, J. Canc. 6 (2015) 759–766.
[25] P.B. Dobrin, Effect of histologic preparation on the cross-sectional area of arterial rings, J. Surg. Res. 61 (1996) 413–415.
[26] R. Kleinloog, E. Korkmaz, J.J. Zwanenburg, et al., Visualization of the aneurysm wall: a 7.0-tesla magnetic resonance imaging study, Neurosurgery 75 (2014) 614–622 discussion 622.
[27] W.H. Bouvy, G.J. Biessels, H.J. Kuijf, et al., Visualization of perivascular spaces and perforating arteries with 7 T magnetic resonance imaging, Invest. Radiol. 49 (2014) 307–313.

[28] M. Mazighi, J. Labreuche, F. Gongora-Rivera, et al., Autopsy prevalence of intracranial atherosclerosis in patients with fatal stroke, Stroke 39 (2008) 1142–1147.
[29] S.C. van den Oord, E.J. Sijbrands, G.L. ten Kate, et al., Carotid intima-media thickness for cardiovascular risk assessment: systematic review and meta-analysis, Atherosclerosis 228 (2013) 1–11.
[30] C.D. Maroules, E. Rosero, C. Ayers, et al., Abdominal aortic atherosclerosis at MR imaging is associated with cardiovascular events: the Dallas heart study, Radiology 269 (2013) 84–91.
[31] A.E. Li, I. Kamel, F. Rando, et al., Using MRI to assess aortic wall thickness in the multiethnic study of atherosclerosis: distribution by race, sex, and age, AJR Am. J. Roentgenol. 182 (2004) 593–597.
[32] L.R. Caplan, P.B. Gorelick, D.B. Hier, Race, sex and occlusive cerebrovascular disease: a review, Stroke 17 (1986) 648–655.
[33] K. Ritz, N.P. Denswil, O.C. Stam, et al., Cause and mechanisms of intracranial atherosclerosis, Circulation 130 (2014) 1407–1414.
[34] S. Gao, R. van 't Klooster, A. Brandts, et al., Quantification of common carotid artery and descending aorta vessel wall thickness from MR vessel wall imaging using a fully automated processing pipeline, J. Magn. Reson. Imag. 45 (2017) 215–228.
[35] D.F. van Wijk, A.C. Strang, R. Duivenvoorden, et al., Increasing spatial resolution of 3T MRI scanning improves reproducibility of carotid arterial wall dimension measurements, Magma 27 (2014) 219–226.